Journal of
Polymer Materials

Tech Science Press

https://doi.org/10.32604/jpm.2026.077474

ARTICLE

Synergistic Therapy of Knee Osteoarthritis Using Amphiphilic ROS-Responsive Nanoparticles Loaded with Celecoxib

Qing Yang[1], **Yi Yang**[2,*] **and Jia Yang**[3,*]

[1]Orthopedics Department, West China School of Public Health and West China Fourth Hospital, Sichuan University, Chengdu, China
[2]Department of Orthopedics, The First Affiliated Hospital of Kunming Medical University, Kunming, China
[3]Department of Orthopedics, Kunming Children's Hospital, Kunming, China

*Corresponding Authors: Yi Yang. Email: yq-1989711@scu.edu.cn; Jia Yang. Email: yunqzh1105@163.com

Received: 10 December 2025; Accepted: 09 April 2026; Published: 30 June 2026

ABSTRACT: The pathological progression of knee osteoarthritis (KOA) is closely associated with synovial inflammation and a microenvironment characterized by excessive reactive oxygen species (ROS). Celecoxib (CEL), a commonly used cyclooxygenase-2 inhibitor suffers from poor targeting and systemic side effects when administered systemically. To achieve precise drug delivery and synergistic therapy at the joint lesion site, this study designed and synthesized an amphiphilic poly (2-oxazoline) block copolymer (POxSP) with a thioketal-based ROS-responsive linker. This polymer was used to construct intelligent nanoparticles (POxSP-CEL) loaded with CEL. These nanoparticles self-assembled in aqueous solution to form spherical structures with an average size of approximately 92.3 nm and uniform distribution, exhibiting rapid disassembly and drug release under high ROS conditions. *In vitro* cellular experiments demonstrated that POxSP-CEL was effectively internalized by macrophages. Through a dual synergistic mechanism involving ROS-triggered drug release and ROS consumption by the carrier, it significantly inhibited the expression of pro-inflammatory cytokines (TNF-α, IL-1β, IL-6) and promoted the expression of the anti-inflammatory cytokine IL-10 in lipopolysaccharide-activated macrophages, effectively reversing the macrophage phenotype from pro-inflammatory M1 to anti-inflammatory M2. In a rat KOA model induced by sodium monoiodoacetate (MIA), intra-articular injection of POxSP-CEL significantly ameliorated cartilage degeneration, reduced proteoglycan loss, and decreased the levels of inflammatory factors in joint tissues. Its therapeutic efficacy was markedly superior to that of free CEL and non-responsive nano-formulations, with no observable significant systemic toxicity. This study confirms that the ROS-responsive POxSP-CEL nano-delivery system not only enables targeted and controlled release of CEL in inflamed joints but also exerts a synergistic therapeutic effect by actively regulating the oxidative stress microenvironment and immune cell function, providing a novel strategy with clinical translation potential for the local and efficient treatment of KOA.

KEYWORDS: Knee osteoarthritis; ROS-responsive; nanodrug delivery; celecoxib; macrophage polarization; synergistic therapy

1 Introduction

Knee osteoarthritis (KOA) is a chronic degenerative joint disease characterized by articular cartilage degeneration, synovial inflammation, and subchondral bone remodeling. Its pathogenesis is complex, involving multiple factors such as mechanical stress, inflammation, and metabolism [1,2]. In synovial inflammation, aberrantly activated macrophages play a central regulatory role. They secrete large amounts of pro-inflammatory cytokines such as IL-1β, IL-6, and TNF-α, initiating an inflammatory cascade that

directly drives chondrocyte apoptosis and extracellular matrix degradation, representing a key factor in KOA progression [3,4]. Intra-articular administration of non-steroidal anti-inflammatory drugs (NSAIDs) can alleviate refractory knee pain and inflammatory effusion [5]. However, limitations such as rapid clearance from the joint space, potential damage to articular cartilage, and accelerated joint degeneration may hinder their clinical application [6,7]. Celecoxib (CEL), a selective cyclooxygenase-2 (COX-2) inhibitor, is a commonly used drug for treating KOA pain and inflammation [8]. Nonetheless, its systemic administration is associated with cardiovascular risks, gastrointestinal side effects, and poor joint targeting, limiting its long-term therapeutic efficacy [9]. Therefore, developing a delivery system capable of targeting diseased joints and intelligently releasing drugs in response to the pathological microenvironment is of great significance for improving the therapeutic effect of CEL while reducing its side effects. ROS-responsive drug delivery systems are currently a research hotspot.

Based on functional phenotypes, macrophages are primarily classified into pro-inflammatory M1 and anti-inflammatory M2 types. In KOA synovium, M1 macrophages predominate. They shape and maintain a pro-inflammatory microenvironment by releasing large quantities of pro-inflammatory factors (e.g., TNF-α, IL-1β, IL-6), reactive oxygen species (ROS), and matrix metalloproteinases [10,11]. ROS is not only a key inflammatory mediator, but its overproduction further drives macrophage polarization towards the M1 phenotype, creating a self-reinforcing vicious cycle of inflammation [12]. Studies have shown that modulating ROS levels can regulate macrophage polarization, promoting a shift from M1 to M2 phenotype, thereby alleviating inflammation. Consequently, targeted clearance of excessive ROS within joints to remodel the inflammatory microenvironment and regulate macrophage function has emerged as a potential novel strategy for treating KOA [13,14]. Based on this, ROS-responsive drug delivery systems have attracted significant attention in recent years [15]. Smart materials constructed using ROS-sensitive chemical bonds such as thioether, selenium, or boronic ester can undergo chemical structural transformation in high ROS environments, enabling targeted and controlled drug release [16–19]. Among these, polymer materials with thioether/thioketal as the responsive unit are particularly promising for joint inflammatory diseases, as their oxidation leads to a significant reversal of hydrophilicity/hydrophobicity, efficiently triggering nanoparticle disassembly and drug release [20,21].

This study aimed to design and synthesize an amphiphilic block copolymer, POxSP-CEL, using a thioketal-based ROS-responsive linker. This polymer can self-assemble in aqueous solution to form core-shell structured nanoparticles, with its hydrophobic core efficiently loading celecoxib. When the nanoparticles are delivered to the inflamed joint via intra-articular injection, the high levels of ROS at the lesion site specifically cleave the thioketal bonds, leading to nanoscale disassembly and rapid drug release. This strategy is expected to enhance the targeted accumulation and efficacy of CEL at the lesion site through ROS-responsive drug release, while the carrier material simultaneously consumes excess ROS during the response process, modulating macrophage polarization to achieve a synergistic therapeutic effect.

2 Materials and Methods

2.1 Main Materials and Reagents

Celecoxib (CEL, B24147, purity > 98%) was purchased from Shanghai Yuanye Bio-Technology Co., Ltd. 2,2′-Thiodiethanol, acetone (123-93-3), 4-pentenoic acid (591-80-0), potassium tert-butoxide (865-47-4), 2-chloroethylamine hydrochloride (870-24-6), triethylamine (TEA) (121-44-8), 1-(3-dimethylaminopropyl)-3-ethylcarbodiimide hydrochloride (EDC) (25952-53-8), N-hydroxysuccinimide (NHS) (6066-82-6), photoinitiator 2959 (I2959) (106797-53-9), 2-phenylethanethiol, methyl trifluoromethanesulfonate (MeOTf) (85708-34-5), 2-methyl-2-oxazoline (MeOx) (1120-64-5), dichloromethane (DCM) (75-09-2), tetrahydrofuran (THF) (109-99-9), N,N-dimethylformamide (DMF) (68-12-2), acetonitrile (ACN) (75-05-8), Sodium

monoiodoacetate (MIA) (I2512) and other polymer synthesis monomers and reagents were purchased from Sigma-Aldrich and purified using standard methods before use. Dialysis bags (MWCO 3500 Da) (131192) were purchased from Spectrum Labs. Lipopolysaccharide (LPS, *E. coli* O111:B4) (R30955601), MTT assay kit (V13154), Mouse Monoclonal Antibody IL-1β (MA5-23691), IL-6 (701028), TNF-α (14-7321-81), DiD cell membrane fluorescent dye (C10046), mouse IL-1β (BMS6002-2TEN), IL-6 (BMS603-2), TNF-α (BMS607-3), IL-10 (88-7105-88), inducible nitric oxide synthase (iNOS) (EEL132) and arginase-1 (Arg-1) (BMS2216) ELISA kits were purchased from Thermo Fisher Scientific (USA). Safranin O-Fast Green staining kit (C0621S) were purchased from Beyotime. RAW264.7 mouse monocyte-macrophage cell line and L929 mouse fibroblast cell line were purchased from the Cell Bank of the Chinese Academy of Sciences. All other chemical reagents were of analytical grade, and water was ultrapure water (prepared by Milli-Q system).

2.2 Synthesis and Characterization of the Amphiphilic Block Copolymer POxSP

2.2.1 Synthesis of 2-Butenyl-2-Oxazoline (ButenOx)

4-Pentenoic acid, NHS, and EDC were dissolved in dry DCM, followed by the addition of 2-chloroethylamine hydrochloride and DIPEA. The reaction mixture was stirred at room temperature under nitrogen protection for 48 h. After completion, the mixture was washed with water, the organic layer was dried, then dissolved in dry THF, and potassium tert-butoxide was added. The reaction proceeded at 60°C for 48 h. Purification via reduced-pressure distillation yielded ButenOx as a colorless liquid.

2.2.2 Synthesis of the Amphiphilic Block Copolymer POxSP

Under anhydrous and oxygen-free conditions, a solution of methyl trifluoromethanesulfonate (MeOTf) in acetonitrile was prepared. 2-Methyl-2-oxazoline (MeOx) was then added to the MeOTf solution, and the reaction proceeded at 70°C for 24 h. After cooling to room temperature, ButenOx was added to the mixture, and the reaction continued at 70°C for 48 h. The reaction solution was dialyzed against distilled water for 2 days and then lyophilized to obtain PENOx. PENOx was dissolved in N,N-dimethylformamide (DMF), and nitrogen was bubbled through the solution for 5 min to remove oxygen. Phenylethanethiol and the photoinitiator Irgacure 2959 were added to the reaction mixture. After nitrogen purging, the reaction vial was sealed and irradiated with 365 nm UV light for 60 min. The reaction solution was dialyzed for purification for 2 days and lyophilized to yield POxSP.

2.3 Preparation and Characterization of POxSP-CEL Nanoparticles (NPs)

To obtain celecoxib-loaded nanoparticles (POxSP-CEL and PENOx-CEL), equal masses of POxSP (or PENOx) and celecoxib were co-dissolved in DMSO. The resulting mixture was then added dropwise into deionized water under constant stirring. After 12 h of stirring at ambient temperature, the suspension was dialyzed against deionized water and subsequently passed through a 0.45 μm aqueous filter membrane.

2.3.1 Size and Morphology

The hydrodynamic diameter and polydispersity index (PDI) of the nanoparticles were determined using Dynamic Light Scattering (DLS, Malvern Zetasizer Nano ZS90). For transmission electron microscopy (TEM, Hitachi HT7800) observation, one droplet of the nanoparticle dispersion was deposited onto a carbon-coated copper grid, negatively stained with phosphotungstic acid, and then air-dried at room temperature prior to imaging.

2.3.2 Stability Study

POxSP-CEL nanoparticle solution was stored at 4°C. In parallel, the nanoparticle solution was lyophilized into powder. At multiple time points (days 0, 7, 14, 21, 28, 35, 42, 49, 56, 63, and 70), aliquots were taken to monitor changes in PDI. After one month of storage at –20°C, the lyophilized powder was reconstituted, and both particle size and PDI were measured to evaluate freeze-drying and reconstitution stability.

2.4 In Vitro ROS-Responsive Drug Release Study

Drug release profiles were assessed using a dialysis bag-based method. Briefly, POxSP-CEL nanoparticle solution containing containing 1 mg of celecoxib was placed in a pre-treated dialysis bag (MWCO 3500 Da). The sealed bag was then placed into phosphate-buffered saline (PBS, pH 7.4) containing 0 M, 100 μM, 0.1 M, or 0.5 M H_2O_2, with 0.5% Tween-80 added to maintain sink conditions. The system was incubated at 37°C with shaking at 100 rpm. At predetermined time points (0.5, 1, 2, 4, 8, 12, 24, 48, 60, 72 h), 1 mL of the external release medium was withdrawn and replaced with an equal volume of fresh pre-warmed medium. Samples were filtered through a 0.22 μm membrane, and CEL concentration was determined using High-Performance Liquid Chromatography (HPLC, Agilent 1260 Infinity II). Chromatographic conditions: C18 reverse-phase column (4.6 mm × 150 mm, 5 μm), mobile phase acetonitrile:water:glacial acetic acid (55:45:0.1, v/v/v), flow rate 1.0 mL/min, detection wavelength 254 nm. Prior to HPLC injection, the nanoparticle solution was demulsified using acetonitrile. Drug concentrations were calculated from a standard curve, and the cumulative release percentage was determined. All release experiments were conducted in triplicate.

2.5 Cell Experiments

2.5.1 Cell Culture

RAW264.7 and L929 cells were cultured in high-glucose DMEM medium supplemented with 10% fetal bovine serum (FBS) and 1% penicillin-streptomycin in a 37°C, 5% CO_2 incubator.

2.5.2 Cell Viability Assay (MTT)

Cells at the logarithmic growth phase were seeded into 96-well plates at a seeding density of 5×10^3 cells/well and allowed to attach for 24 h. Subsequently, the culture medium was exchanged with fresh medium containing varying concentrations (0.125, 0.25, 0.5, and 1 mg/mL) of POxSP, PENOx, POxSP-CEL, PENOx-CEL, or an equivalent amount of free CEL (dissolved in DMSO, final concentration < 0.1%). Untreated cells served as the negative control. Following an additional 24 h incubation, 20 μL of MTT solution (5 mg/mL) was added to each well, followed by 4 h of further incubation. The supernatant was then removed, and 150 μL of DMSO was added to dissolve the formazan crystals. The absorbance (OD value) was measured at 490 nm using a microplate reader (BioTek Synergy H1). Cell viability was calculated as (OD_experimental/OD_control) × 100%.

2.5.3 Cellular Uptake Assay

POxSP-CEL nanoparticles were labeled with the fluorescent dye DiD (1 μg/mL) by incubation in the dark for 30 min, followed by ultrafiltration centrifugation to remove free dye. RAW264.7 cells were seeded into confocal dishes. After adherence, DiD-labeled POxSP-CEL (1 mg/mL) was added. After incubation for 1, 2, and 4 h, cells were washed three times with pre-cooled PBS, fixed with 4% paraformaldehyde, and nuclei were stained with DAPI. Intracellular fluorescence was observed using a confocal laser scanning microscope

(CLSM, Leica TCS SP8), and the mean fluorescence intensity (MFI) was quantitatively analyzed by flow cytometry (BD FACSCanto II).

2.5.4 Intracellular ROS Scavenging Assay

The intracellular ROS scavenging capability of POxSP-based nanoparticles was evaluated using the 2′,7′-dichlorodihydrofluorescein diacetate (DCFH-DA) fluorescent probe. RAW 264.7 macrophages were seeded in 6-well plates at a density of 2 × 1052 × 105 cells/well and cultured for 24 h. To simulate the inflammatory microenvironment, the cells were stimulated with lipopolysaccharide (LPS, 1 μg/mL) for 12 h to induce excessive ROS production. Subsequently, the medium was replaced with fresh medium containing POxSP or POxSP-CEL (at an equivalent polymer concentration) and incubated for another 6 h. After treatment, the cells were washed three times with PBS and incubated with 10 μM DCFH-DA in serum-free medium at 37°C for 30 min in the dark. After being washed thoroughly to remove extracellular probes, the cells were collected, resuspended in PBS, and analyzed using a flow cytometer (BD FACSCanto II, USA).

2.5.5 Cell Apoptosis Analysis

Apoptosis was evaluated with an Annexin V-FITC/PI kit (Beyotime) per the manufacturer's instructions. RAW264.7 cells (2×10^5/well in 6-well plates, 24 h attachment) were treated with LPS (1 μg/mL) plus PBS (control), blank POxSP, free CEL, or POxSP-CEL (10 μg/mL CEL equivalent) for 24 h. Cells were trypsinized (no EDTA), centrifuged (1500 rpm, 5 min), washed with cold PBS, and resuspended in 100 μL 1 × Binding Buffer. Annexin V-FITC (5 μL) and PI (5 μL) were added (15 min, dark, room temperature). After adding 400 μL Binding Buffer, samples were analyzed by flow cytometry (≥10,000 events/sample). Apoptotic cells (Annexin V^+/PI^- plus Annexin V^+/PI^+) were quantified using FlowJo.

2.5.6 Cytokine Expression Analysis

RAW264.7 cells (1×10^5/well in 12-well plates, 24 h) were assigned to seven groups: control (no LPS), LPS model (1 μg/mL LPS alone), LPS + POxSP, LPS + PENOx, LPS + POxSP-CEL, LPS + PENOx-CEL, and LPS + free CEL (drug doses equal to CEL content in 1 mg/mL POxSP-CEL). Except controls, all groups received LPS for 6 h to activate macrophages. The medium was then replaced with fresh medium containing the indicated treatments for another 18 h. Supernatants were harvested, and levels of TNF-α, IL-1β, IL-6, IL-10, iNOS, and Arg-1 were measured by ELISA (kits used per manufacturer's instructions).

2.6 Animal Experiments

2.6.1 Animals and KOA Model Establishment

All animal experiments were approved by the Orthopedics Department West China School of Public Health and West China Fourth Hospital (approved no. FHSC202519). Eight-week-old healthy male Sprague-Dawley (SD) rats (weight 200 ± 20 g) were randomly divided into 5 groups (n = 8): sham operation group (Control), model + PBS group (PBS), model + free CEL group (CEL), model + POxSP group (POxSP), model + POxSP-CEL group (POxSP-CEL). A unilateral knee KOA model was established by intra-articular injection of sodium monoiodoacetate (MIA): rats were anesthetized by intraperitoneal injection of 1% sodium pentobarbital, and the right knee joint cavity was injected with MIA solution (3 mg in 50 μL saline) [22]. The sham group received an equal volume of saline injection. Treatment began one week after modeling. All rats were purchased from Yunnan Luoyu Biotechnology Co., Ltd., and the experimental facility was licensed under No. SYXK (Dian) K2021-0003.

2.6.2 Administration Regimen

Rats in the treatment groups received intra-articular injections (50 μL/injection) on days 7, 14, and 21 post-induction. To ensure consistent dosing, the amount of celecoxib was normalized to 100 μg per injection for both the free drug and nanoparticle formulations. Specifically, for the CEL group, due to the hydrophobic nature of celecoxib, the drug was dissolved in saline containing a biocompatible co-solvent [DMSO/Tween-80] and sonicated to form a uniform suspension. The POxSP and POxSP-CEL groups were administered drug-loaded nanoparticle aqueous solutions, respectively. The PBS group received an equivalent volume of saline, while the Sham group remained untreated.

2.6.3 Sample Collection and Processing

Seven days after the last administration (i.e., day 28 after modeling), rats were anesthetized, blood was collected via cardiac puncture to obtain serum for biochemical analysis. Subsequently, rats were euthanized, and the right knee joints were completely dissected and fixed in 4% paraformaldehyde for 48 h for subsequent histological analysis.

2.7 Histological and Immunohistochemical Analysis

Fixed knee joint specimens were decalcified in 10% EDTA for 4 weeks, dehydrated through a graded ethanol series, and embedded in paraffin. Serial sagittal sections (5 μm thickness) were prepared.

2.7.1 Hematoxylin and Eosin (H&E) Staining and Safranin O-Fast Green Staining

Performed according to standard protocols to assess synovial inflammation, cartilage structure, and proteoglycan content. The Osteoarthritis Research Society International (OARSI) scoring system was used for semi-quantitative blinded scoring of articular cartilage degeneration.

2.7.2 Immunohistochemistry (IHC)

After antigen retrieval, blocking of endogenous peroxidase, and serum blocking, sections were incubated overnight at 4°C with primary antibodies (rabbit anti-rat IL-1β, IL-6, TNF-α, 1:200 dilution). The next day, sections were incubated with HRP-labeled secondary antibodies at room temperature for 1 h, developed with DAB, and counterstained with hematoxylin. Image-Pro Plus software was used to analyze the mean optical density (MOD) of positive staining in the articular cartilage region.

2.8 Safety Evaluation

Potential liver and kidney toxicity was assessed by measuring serum levels of BUN, Cre, ALT, and AST via an automatic biochemical analyzer.

2.9 Statistical Analysis

Data are shown as mean ± SD ($x \pm s$). Statistical evaluation was conducted with GraphPad Prism 9.0. Multiple group comparisons were performed using one-way ANOVA, followed by Tukey's post-hoc test (if variances were homogeneous) or the Games-Howell test (if not). Two-group comparisons were made via independent samples *t*-test. Significance was set at $p < 0.05$.

3 Results

3.1 Synthesis, Characterization, and ROS Responsiveness of POxSP

To construct the intelligent delivery system, the amphiphilic block copolymer POxSP with a thioketal responsive unit was first successfully synthesized. The ^{1}H NMR spectrum (Fig. 1A) indicated signals belonging to the thioketal structure (-SCH_2-, δ 2.75 ppm) and the benzyl group (δ 7.61 ppm), confirming the chemical structure of the target polymer. This polymer can self-assemble in aqueous solution to form nanoparticles (POxSP-CEL) loaded with celecoxib (CEL). Dynamic light scattering (DLS) and transmission electron microscopy (TEM) characterization (Fig. 1B,C) showed that POxSP-CEL exhibited a regular spherical shape with a hydrodynamic diameter of (92.3 ± 5.6) nm and good dispersity (PDI~0.21). The nano-formulation maintained stable size and PDI for over two months during storage at 4°C and after lyophilization/reconstitution (Fig. 1D), indicating good physical stability. *In vitro* release studies are shown in Fig. 1E. The drug release of POxSP-CEL exhibited a clear H_2O_2-responsive behavior, with the cumulative release rate of CEL being positively correlated with the H_2O_2 concentration. At physiological pH (PBS, pH 7.4), POxSP-CEL demonstrated excellent stability with minimal premature leakage, as only approximately 25% of the encapsulated CEL was released over 48 h. This suggests that the carrier effectively sequesters the drug under physiological conditions. To evaluate the ROS-triggered release, H_2O_2 concentrations were established at 100 μM to simulate pathologically relevant levels in the inflammatory micro-environment [23], while 0.1 M and 0.5 M H_2O_2 concentrations served as accelerated release models to validate the sensitivity of the ROS response. At 100 μM H_2O_2, the acceleration of drug release was initially subtle within the first 24 h (23.2% vs. 18.7% in PBS). However, a significant divergence was observed by 60 h, with the cumulative release reaching 42.6%, which was markedly higher than that of the PBS control (26.1%). Under accelerated conditions (0.1 M H_2O_2 and 0.5 M H_2O_2), the drug release rate increased drastically. Notably, in the presence of 0.5 M H_2O_2, the cumulative release exceeded 80% within 24 h. These results collectively underscore the superior ROS-responsiveness of the POxSP-CEL nanoparticles and their capability for triggered cargo release in oxidative environments.

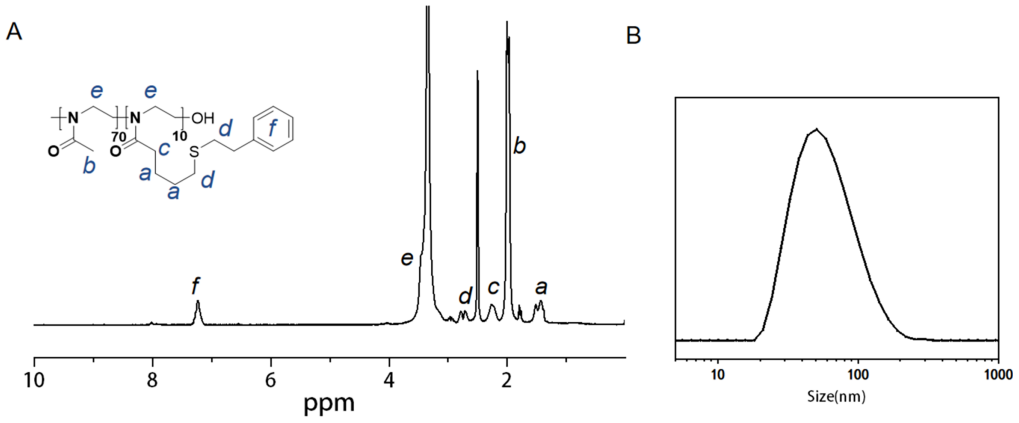

Figure 1: (Continued)

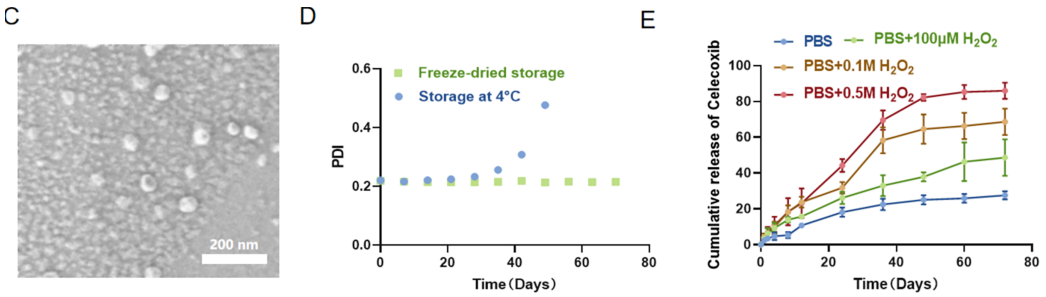

Figure 1: Synthesis, characterization, and ROS responsiveness of POxSP. (**A**) ^{1}H NMR spectrum of POxSP, showing characteristic peaks of the thioketal unit (-SCH_2- at δ 2.75 ppm) and the phenyl group (δ 7.61 ppm). (**B**) Dynamic light scattering (DLS) analysis of POxSP-CEL nanoparticles, indicating a hydrodynamic diameter of approximately 92.3 nm. (**C**) Transmission electron microscopy (TEM) image of POxSP-CEL nanoparticles, demonstrating spherical morphology and uniform distribution. (**D**) Stability of POxSP-CEL nanoparticles stored at 4°C and after lyophilization/reconstitution over 70 days, as assessed by polydispersity index (PDI). (**E**) *In vitro* drug release profile of POxSP-CEL under different H_2O_2 concentrations (0 M, 100 μM, 0.1 M, 0.5 M) simulating physiological and high-ROS environments. Data are presented as mean ± SD (n = 3).

3.2 In Vitro Biocompatibility, Cellular Uptake, and ROS Scavenging Capability

Evaluating the cytocompatibility and targeting of nanoparticles is fundamental for advancing their application. The MTT assay showed (Fig. 2A) that even at concentrations as high as 1 mg/mL, POxSP, the non-responsive carrier PENOx, and POxSP-CEL showed no significant cytotoxicity towards mouse fibroblast cells (L929) ($p > 0.05$). However, a different trend was observed in RAW264.7 macrophages (Fig. 2B). Compared to PENOx, POxSP and POxSP-CEL inhibited macrophage proliferation viability in a concentration-dependent manner ($p < 0.05$). Moreover, the inhibitory effect of CEL-loaded POxSP-CEL was significantly stronger than that of the blank carrier POxSP ($p < 0.05$), suggesting its stronger anti-inflammatory/anti-proliferative effect.

As shown in Fig. 2C,D, DiD fluorescent dye-labeled POxSP-CEL could rapidly bind to and be internalized by RAW264.7 cells. Significant intracellular fluorescence could be detected after 1 h of incubation, and the fluorescence intensity significantly increased with prolonged incubation time (up to 12 h) ($p < 0.05$). This proves that POxSP-CEL can be efficiently taken up by macrophages, creating conditions for subsequent intracellular response and pharmacological effects. The intracellular ROS scavenging capability of the carrier was then evaluated using the DCFH-DA probe (Fig. 2E). Upon LPS stimulation, macrophages exhibited a dramatic increase in ROS levels; however, treatment with POxSP and POxSP-CEL effectively quenched the ROS-driven fluorescence, demonstrating the potent antioxidant activity of the thioketal-based carrier.

To further distinguish whether the decreased viability observed in Fig. 2B was due to targeted pharmacological action or non-specific carrier toxicity, an Annexin V-FITC/PI apoptosis assay was performed (Fig. 2F). The blank carrier POxSP showed negligible levels of apoptosis and necrosis (1.7%), comparable to the PBS control group (1.2%), demonstrating the excellent biocompatibility of the copolymer scaffold. In contrast, POxSP-CEL induced a significantly higher total apoptosis rate (12.5%) compared to free CEL (6.1%). Notably, the necrosis rate (PI single positive) remained extremely low across all groups, indicating that the enhanced growth inhibition in RAW264.7 cells was primarily driven by programmed apoptosis rather than non-specific toxic necrosis. These results prove that POxSP-CEL can efficiently enter macrophages, neutralize intracellular ROS, and trigger programmed cell death to eliminate over-activated inflammatory cells.

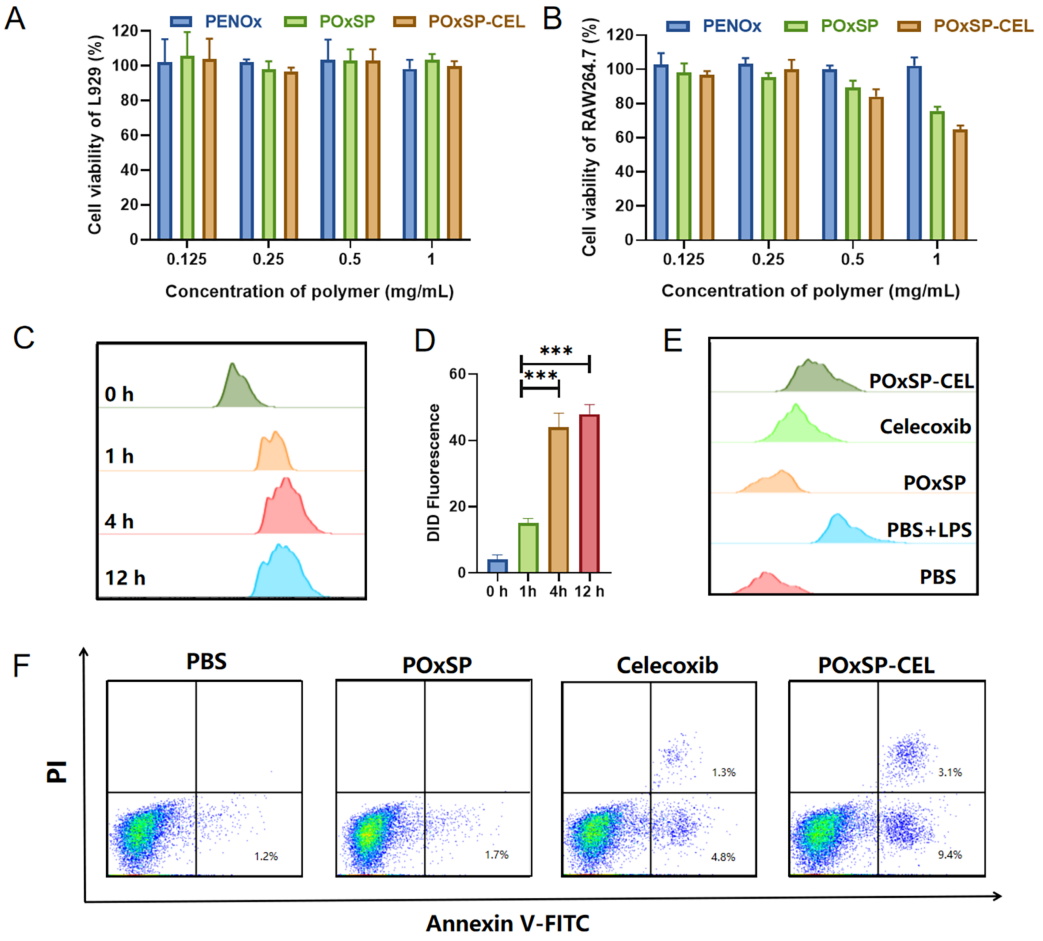

Figure 2: *In vitro* biocompatibility, cellular uptake, and ROS scavenging capacity of POxSP-CEL. (**A**) Cell viability of L929 fibroblasts after 24 h exposure to PENOx, POxSP, and POxSP-CEL at various concentrations (0.125–1 mg/mL) measured by MTT assay. (**B**) Cell viability of RAW264.7 macrophages under the same treatment conditions. (**C**) Flow cytometry histograms and (**D**) quantitative analysis of mean fluorescence intensity (MFI) showing the time-dependent cellular uptake of DiD-labeled POxSP-CEL by RAW264.7 cells at 0, 1, 4, and 12 h. (**E**) Intracellular ROS scavenging capability in LPS-activated RAW264.7 cells after different treatments, as determined by DCFH-DA fluorescent probe using flow cytometry. (**F**) Representative Annexin V-FITC/PI flow cytometry plots of RAW264.7 cells after treatment with PBS, POxSP, Celecoxib, and POxSP-CEL for 24 h, showing the percentages of apoptotic (Q3) and necrotic (Q2) cells. Data are presented as mean ± SD (n = 3, ***$p < 0.001$).

3.3 Regulatory Effect of POxSP-CEL on the Inflammatory Phenotype of Activated Macrophages

Based on its favorable uptake characteristics, we further investigated the regulatory capacity of POxSP-CEL on macrophage inflammatory polarization. After LPS stimulation, RAW264.7 cells were successfully activated to the M1 phenotype, manifested by significantly upregulated expression of pro-inflammatory factors (TNF-α, IL-1β, IL-6) and M1 marker (iNOS), while the expression of the anti-inflammatory factor IL-10 and M2 marker (Arg-1) was downregulated (Fig. 3). In this model, the non-responsive carrier PENOx had no significant effect on the cytokine profile ($p < 0.05$). In contrast, POxSP-CEL treatment exhibited the strongest anti-inflammatory and phenotype-reprogramming effects: it could extremely significantly inhibit the LPS-induced high expression of TNF-α, IL-1β, IL-6, and iNOS, while significantly elevating the levels of IL-10 and Arg-1 ($p < 0.01$). Furthermore, the effect of POxSP-CEL was superior to that of an equivalent dose of free CEL, the non-responsive drug-loaded nanoparticle PENOx-CEL, and also superior

to the blank ROS-responsive carrier POxSP. These findings provide compelling evidence that POxSP-CEL achieves more than simple anti-inflammatory inhibition. The significant downregulation of iNOS and the concurrent upregulation of Arg-1 (a classic functional marker of the M2 phenotype) indicate a fundamental shift in macrophage polarization. This phenotypic reversal is driven by a dual synergistic mechanism: the POxSP carrier first 'pre-conditions' the microenvironment by scavenging intracellular ROS—a primary driver of M1 polarization—thereby lowering the activation threshold. Subsequently, the ROS-triggered release of CEL suppresses the downstream inflammatory cascade at its source. By effectively reprogramming synovial macrophages from a catabolic M1 state to a reparative M2 state, POxSP-CEL curtails the production of matrix-degrading enzymes and pro-apoptotic cytokines. This systemic remodeling of the immune microenvironment serves as a critical prerequisite for the subsequent preservation of articular cartilage structure and the reduction of OARSI scores observed in our *in vivo* models. The results suggest that POxSP-CEL effectively reverses the macrophage phenotype from pro-inflammatory M1 to reparative M2.

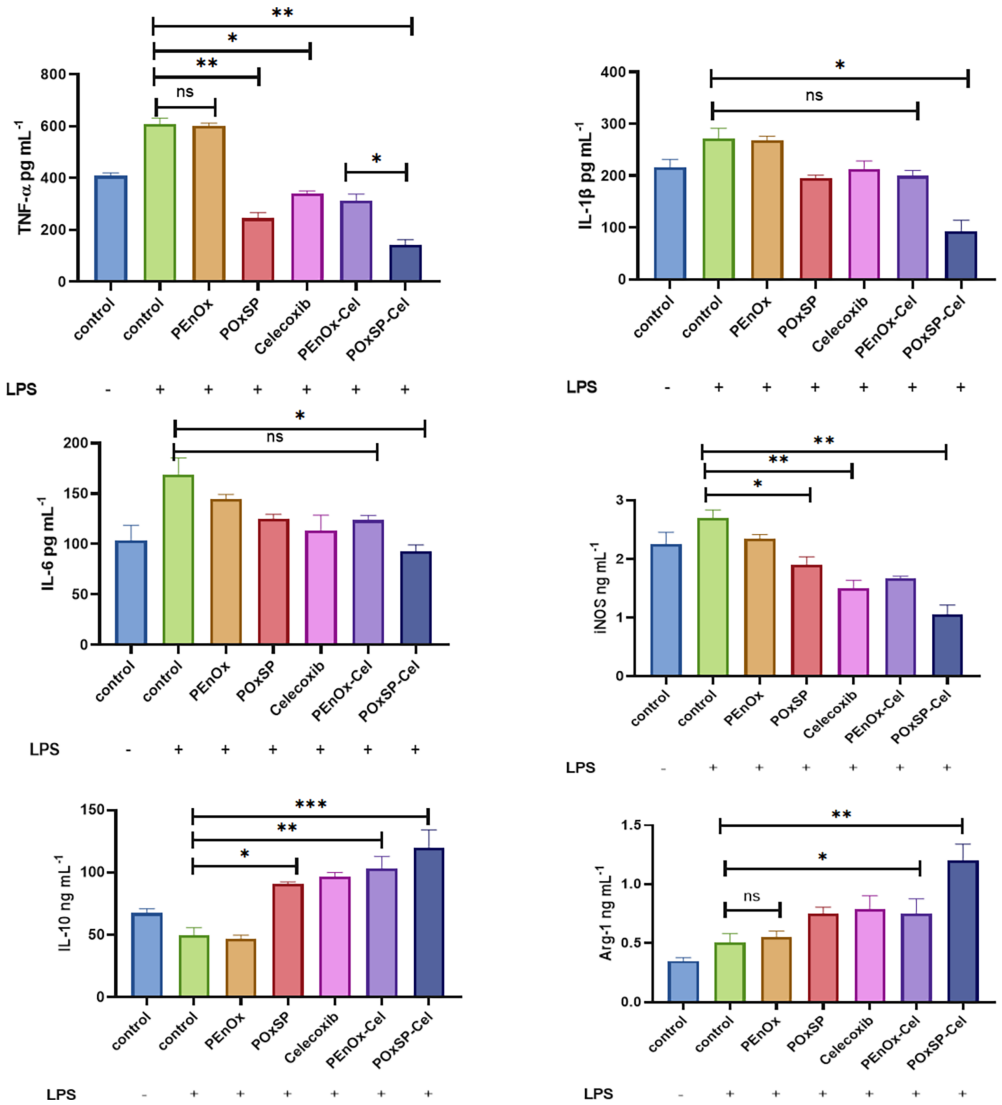

Figure 3: Regulation of macrophage inflammatory polarization by POxSP-CEL. Data are presented as mean ± SD. Group comparisons were performed using one-way ANOVA followed by Tukey's post-hoc test. Significance levels are denoted by asterisks: $^{*}p < 0.05$, $^{**}p < 0.01$, $^{***}p < 0.001$. No significant difference is indicated by "ns" ($p \geq 0.05$).

3.4 Therapeutic Efficacy of POxSP-CEL in a Rat KOA Model

To verify *in vivo* efficacy, we established a rat KOA model induced by MIA. Histopathological analysis (Fig. 4A) showed that compared to the sham operation group (Control), the model group (PBS) exhibited severely damaged articular cartilage surface, thinning of the cartilage layer, substantial loss of proteoglycans as indicated by Safranin O staining, and a significantly increased OARSI score (Fig. 4B). Concurrently, immunohistochemistry (IHC) showed a sharp rise in the expression levels of IL-1β, IL-6, and TNF-α in cartilage tissue (Fig. 4C–E) ($p < 0.01$). Intra-articular injection of free CEL or the blank carrier POxSP alleviated cartilage degeneration and inflammation to some extent, but the improvement was limited. In contrast, the POxSP-CEL treatment group showed nearly complete protective effects: the cartilage surface was smoothest, cartilage thickness and proteoglycan content were closest to normal, and the OARSI score was significantly lower than all other treatment groups ($p < 0.01$). IHC results further confirmed that the expression of pro-inflammatory cytokines in the articular cartilage of the POxSP-CEL group was most effectively suppressed. These data indicate that POxSP-CEL can achieve cartilage protection and anti-inflammatory effects by targeting the joint cavity and responding to the inflammatory microenvironment.

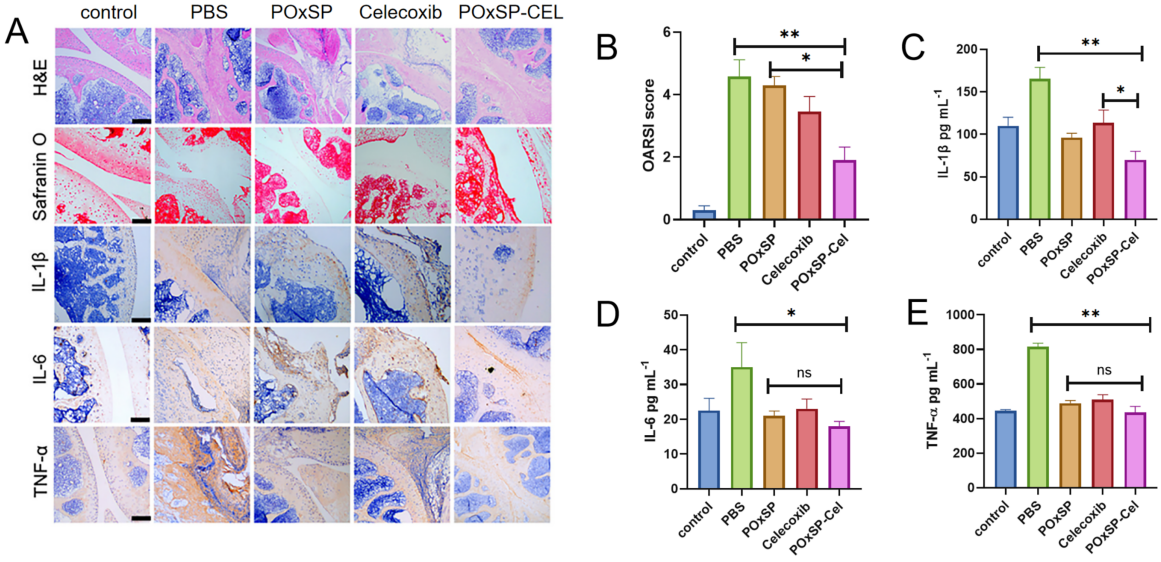

Figure 4: Therapeutic efficacy of POxSP-CEL in a rat KOA model. (**A**) Representative images of H&E and Safranin O-Fast Green staining of articular cartilage from different treatment groups: Control (sham), PBS (model), free CEL, POxSP, and POxSP-CEL. Scale bar: 100 μm. (**B**) OARSI scores for cartilage degeneration in each group. Immunohistochemical staining and mean optical density (MOD) analysis of IL-1β (**C**), IL-6 (**D**), and TNF-α (**E**) in articular cartilage. Data are mean ± SD (n = 8 rats/group). Data are presented as mean ± SD. Group comparisons were performed using one-way ANOVA followed by Tukey's post-hoc test. Significance levels are denoted by asterisks: $^{*}p < 0.05$, $^{**}p < 0.01$. No significant difference is indicated by "ns" ($p \geq 0.05$).

3.5 Systemic Safety Evaluation of POxSP-CEL

To ensure the safety of the therapeutic strategy, we examined the serum biochemical indicators of the treated rats. The results showed no statistically significant differences ($p > 0.05$) in the levels of blood urea nitrogen (BUN), creatinine (Cre), alanine aminotransferase (ALT), and aspartate aminotransferase (AST) among all experimental groups (including the high-dose POxSP-CEL treatment group), and all values were within the normal range (Fig. 5). This indicates that under the administration regimen used in this study, the POxSP-CEL nano-system did not cause detectable liver or kidney function damage, demonstrating good systemic safety.

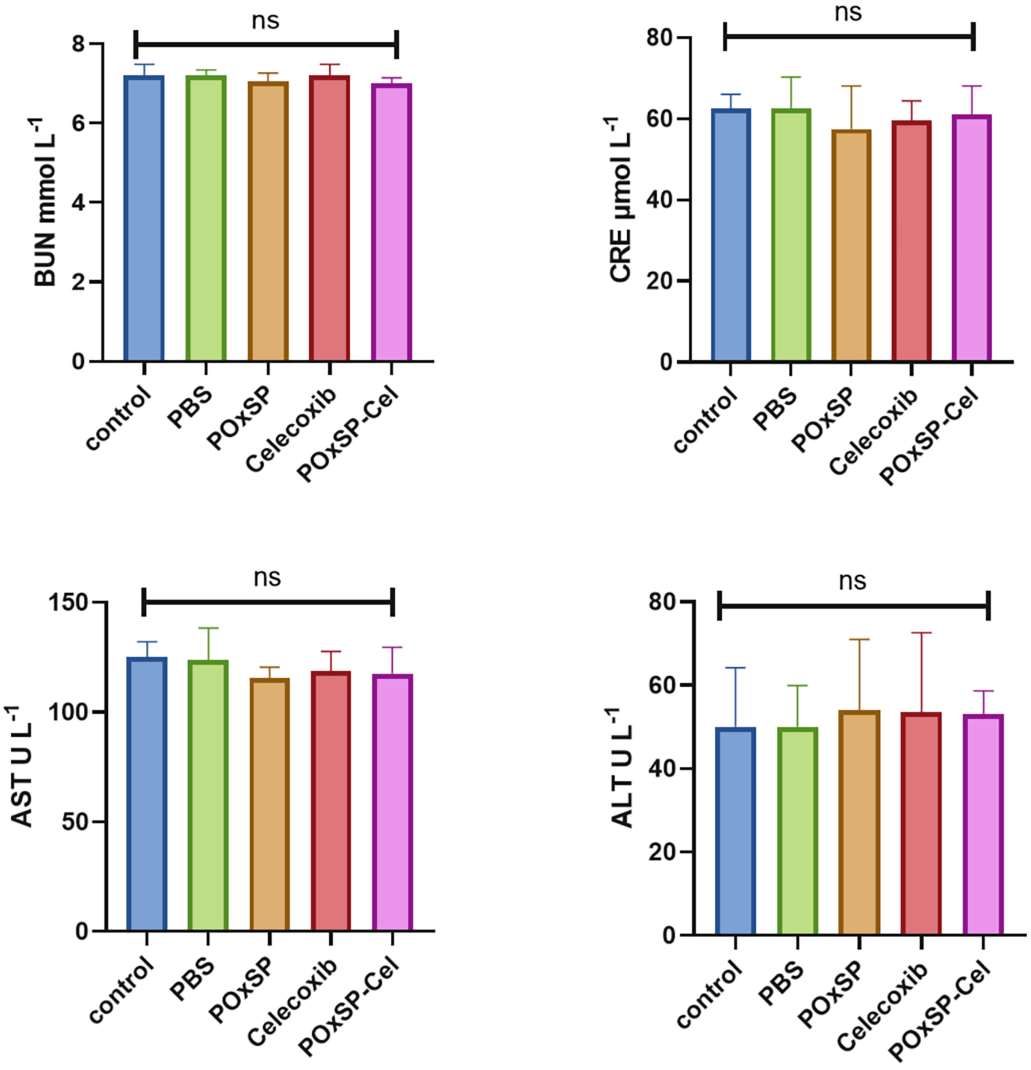

Figure 5: Systemic safety evaluation of POxSP-CEL in a rat KOA model. No significant difference is indicated by "ns" ($p \geq 0.05$).

4 Discussion

As a chronic, progressive joint disease, the core of KOA treatment lies in effectively controlling synovial inflammation, blocking the cartilage destruction cascade, while avoiding systemic toxicity [14,24]. This study successfully designed and constructed an amphiphilic block copolymer, POxSP, based on a thioketal ROS-responsive linker, and used it as a carrier to load celecoxib, forming an intelligent nano-delivery system, POxSP-CEL. This system not only achieved ROS-triggered precise drug release at the inflammatory joint site in KOA but also synergistically regulated macrophage polarization through the carrier material's own ROS scavenging ability. Ultimately, it demonstrated synergistic therapeutic effects superior to traditional administration methods in both *in vitro* and *in vivo* models. This study provides a novel strategy with translational potential for the targeted and synergistic treatment of KOA.

Traditional nanodrug delivery systems often focus on improving drug solubility or prolonging circulation time, with limited ability to actively respond to and intervene in the pathological microenvironment. Drawing from and developing the concept proposed by Simon et al. that amphiphilic poly (2-oxazoline)s

enable efficient intracellular delivery, we developed the key responsive unit-based POxSP copolymer [25]. ^{1}H NMR and *in vitro* release experiments (Fig. 1A,E) confirmed its chemical structure and its ability to rapidly disassemble and release drugs in high ROS environments. This design means that CEL release no longer relies solely on passive diffusion but is triggered and regulated by the excessive ROS expressed in KOA synovial fluid. When nanoparticles accumulate at the inflammatory site, locally high levels of ROS cleave the thioketal bonds, achieving burst release of the drug, thereby significantly increasing the local drug concentration at the lesion. Simultaneously, the oxidation of thioketal to hydrophilic sulfone or sulfoxide is itself a chemical reaction that consumes ROS. This means that POxSP-CEL, while releasing the drug, directly reduces the oxidative stress level in the pro-inflammatory microenvironment. Crucially, this intrinsic ROS-scavenging capability functions as a "sacrificial antioxidant" mechanism [26], effectively depleting the local ROS pool that typically drives synovial macrophages toward the pro-inflammatory M1 phenotype [27]. This establishes a synergistic therapeutic loop: the carrier "pre-conditions" the microenvironment by lowering the oxidative threshold, thereby potentiating the efficacy of the released CEL in suppressing downstream inflammatory cytokines.

The experimental results of this study showed that the inhibitory effect of POxSP-CEL on macrophage proliferation was significantly stronger than that of non-responsive PENOx-CEL and free CEL (Fig. 2B), and it could be efficiently internalized by macrophages (Fig. 2C,D), laying the foundation for its intracellular action. To further investigate the mechanism of this enhanced efficacy, we evaluated the intracellular ROS scavenging capability of the carrier. As shown in Fig. 2E, the POxSP-based nanoparticles effectively quenched the high levels of ROS in LPS-activated macrophages, confirming that the thioketal-containing carrier directly participates in restoring the redox balance. To confirm that this enhanced inhibition was a desired pharmacological outcome rather than non-specific carrier toxicity, we further analyzed the mode of cell death using Annexin V-FITC/PI staining (Fig. 2F). The blank carrier POxSP showed negligible apoptosis and necrosis (1.7%), comparable to the PBS control (1.2%), which validates the high biocompatibility of the poly (2-oxazoline)-based scaffold. In contrast, POxSP-CEL induced a significantly higher rate of programmed apoptosis (12.5%) than free CEL (6.1%), while the necrosis rate remained extremely low across all groups. These results demonstrate that the ROS-responsive nanoparticles leveraging the phagocytic nature of activated macrophages to achieve high intracellular drug concentrations and trigger programmed cell death, thereby effectively reducing the pro-inflammatory cell population without causing toxic side effects.

While our results confirm robust uptake by macrophages, the degree of preferential targeting toward M1 macrophages over other cell populations, such as M2 macrophages and synovial fibroblasts, remains a subject for further refinement. Generally, activated M1 macrophages exhibit significantly higher phagocytic activity than other synovial cells, which inherently facilitates the accumulation of nanoparticles in these pro-inflammatory cells [28]. More importantly, the ROS-responsive design of our carrier provides a "functional targeting" mechanism. Since M1 macrophages are the primary source of ROS in the inflamed joint, the high concentration of ROS not only triggers drug release but is also simultaneously neutralized by the carrier itself (Fig. 2E). because M1 macrophages are the predominant producers of reactive oxygen species in the osteoarthritic joint, the thioketal linkers are more likely to be cleaved within these specific cells, leading to localized drug release [29]. The combination of efficient scavenging of pro-inflammatory ROS and the induction of targeted apoptosis (Fig. 2F) explains why POxSP-CEL exhibits superior therapeutic potential compared to free drugs. However, we acknowledge as a limitation that our current carrier lacks active targeting ligands. Future studies will explore the conjugation of M1-specific moieties to the poly (2-oxazoline) backbone to further enhance the precision of this delivery platform.

In the LPS-induced macrophage activation model, POxSP-CEL exhibited anti-inflammatory and phenotype-regulating functions (Fig. 3). The effect of POxSP-CEL was significantly superior to that of

the drug alone (free CEL) or the carrier alone (POxSP). POxSP-CEL could most effectively downregulate the expression of key pro-inflammatory factors (TNF-α, IL-1β, IL-6) and the M1 marker (iNOS), while significantly upregulating the expression of the anti-inflammatory factor IL-10 and the M2 marker (Arg-1). The POxSP carrier consumes intracellular ROS during the response process and reverses the ROS-driven polarization of macrophages towards the M1 phenotype. This reprograms macrophages from the pro-inflammatory M1 phenotype to the reparative M2 phenotype, thereby suppressing the inflammatory cascade at its source, highlighting the unique advantage of drug-carrier synergy.

Histological scoring (OARSI score) and staining results (Fig. 4) consistently indicated that the POxSP-CEL treatment group had the best effect in protecting cartilage structure and maintaining proteoglycan content, almost restoring to the level of the sham group. Immunohistochemical analysis further showed that the expression of IL-1β, IL-6, and TNF-α in the articular cartilage of this group was most potently inhibited. This *in vivo* efficacy can be attributed to: (1) Retention advantage after intra-articular injection: The nanoscale size (~92 nm) facilitates retention within the joint cavity, avoiding rapid clearance by synovial lymphatic vessels and prolonging the duration of action [30]. (2) Lesion targeting and intelligent drug release: In the high ROS microenvironment surrounding inflamed synovium and activated macrophages, POxSP-CEL specifically disassembles, achieving targeted enrichment of CEL at the lesion site, improving local bioavailability, and reducing off-target effects on normal tissues. (3) Microenvironment remodeling: The carrier continuously consumes excessive ROS within the joint cavity, not only directly reducing oxidative damage but also, by regulating synovial macrophage polarization, creating a local immune microenvironment conducive to cartilage repair.

Finally, systematic safety assessment preliminarily confirmed the good biocompatibility of this nano-formulation. Serum biochemical indicators showed that POxSP-CEL did not cause significant liver or kidney function damage (Section 3.5 of Results). While this study focuses on the short-term therapeutic efficacy and safety, the long-term fate of the POxSP carrier is a critical consideration. The POxSP-CEL nanoparticles are designed to disassemble upon triggering by ROS in the OA joint. The resulting POx fragments, with a molecular weight below the renal threshold, are expected to be cleared via lymphatic drainage from the joint and subsequent renal excretion, as supported by previous studies on POx-based therapeutics [31]. *In vitro* cytotoxicity experiments also indicated no significant toxicity towards fibroblast L929 cells (Fig. 2A). In normal tissues (low ROS environment), the nanoparticles remain stable, drugs are released slowly, and the carrier material is inert; they are only activated at the lesion site (high ROS environment), thereby maximizing the reduction of systemic side effects and potential long-term toxicity risks of the carrier material while improving efficacy.

This study has certain limitations. First, although the animal model (MIA-induced) can simulate KOA pain and cartilage degeneration, it differs from the complex chronic course of human KOA. Second, the long-term *in vivo* degradation fate, immunogenicity, and more extensive toxicological evaluation of the nanoparticles require further in-depth study. Future work will focus on: (1) Exploring nanoparticle surface functionalization (e.g., with specific ligands targeting synovium or M1 macrophages) to further enhance targeting efficiency; (2) Loading other drugs with cartilage-protective effects (e.g., growth factors, small molecule inhibitors) to construct multi-drug synergistic systems; (3) Conducting efficacy evaluation in large animal models (e.g., spontaneous OA in dogs) to lay a more solid foundation for clinical translation.

5 Conclusion

This study successfully developed a ROS-responsive intelligent nano-delivery system, POxSP-CEL. POxSP-CEL, through its dual synergistic mechanism of triggered drug release and microenvironment regulation, efficiently inhibits synovial inflammation, regulates macrophage polarization, protects articular

cartilage, and demonstrates excellent therapeutic efficacy and good safety in animal models. This work not only provides a safer and more efficient novel local joint delivery formulation for celecoxib but also offers new ideas for a theranostic nanoplatform for the treatment of KOA and other inflammatory diseases.

Acknowledgement: Not applicable.

Funding Statement: The authors received no specific funding for this study.

Author Contributions: The authors confirm contribution to the paper as follows: Conceptualization, Jia Yang and Yi Yang; methodology, Qing Yang; software, Yi Yang; validation, Jia Yang; writing—original draft preparation, Qing Yang; writing—review and editing, Yi Yang and Jia Yang. All authors reviewed and approved the final version of the manuscript.

Availability of Data and Materials: Data available within the article.

Ethics Approval: All animal experiments were approved by the Orthopedics Department West China School of Public Health and West China Fourth Hospital (approved no. FHSC202519).

Conflicts of Interest: The authors declare no conflicts of interest.

References

1. Ye H, Li ZQ, Yang JM, Long Y, Zhong YB, Wu Y, et al. A network pharmacology-based study to investigate the mechanism of curcumin-regulated regenerative repair of quadriceps femoris muscle in KOA rats. Eur J Pharmacol. 2024;982:176910. doi:10.1016/j.ejphar.2024.176910.
2. Wei Y, Ma Z, Li Z, Kang J, Liao T, Jie L, et al. Gentiopicroside ameliorates synovial inflammation and fibrosis in KOA rats by modulating the HMGB1-mediated PI3K/AKT signaling axis. Int Immunopharmacol. 2025;147:113973. doi:10.1016/j.intimp.2024.113973.
3. Li Y, Liao X, Yu X, Xiao Y, Tao X, Zhong T. Mediating role of the ANGPTL3/TFPI protein ratio in regulating T-Cell surface Glycoprotein CD5 levels on Knee Osteoarthritis (KOA): a mendelian randomization study. Int J Mol Sci. 2025;26(10):4471. doi:10.3390/ijms26104471.
4. Wang W, Li T, Zhang J, Guan T, Xu S, Lai Y, et al. Nystose mitigates mono sodium iodoacetate-induced knee osteoarthritis by inhibiting the NLRP3 Inflammasome. Phytomedicine. 2025;150:157598. doi:10.1016/j.phymed.2025.157598.
5. Thomas DT, Eapen C, Hegde AS, Mahale AR, Mane PP, Mehta S. Effectiveness of the core activation and rehabilitation exercises for knee osteoarthritis-program (CARE-KOA©) among patients diagnosed with knee osteoarthritis. F1000Res. 2025;14:496. doi:10.12688/f1000research.163321.1.
6. Yanuarso, Dandan KL, Putranto TA, Sartika CR, Wijaya A, Mulyadi D, et al. The effectiveness of mesenchymal stem cell (MSCs) therapy combined with arthroscopy as treatment for knee osteoarthritis (KOA): a systematic review. Orthop Rev. 2025;17:137660. doi:10.52965/001c.137660.
7. Cheng L, Li GZ, Shen X, Xie Y. Effects of celecoxib combined with glucosamine hydrochloride in the management of knee osteoarthritis. Am J Transl Res. 2025;17(8):6359–69. doi:10.62347/ahto9889.
8. Yang X, Song H, Li X, Wu T, Li J, He C. Neuromuscular exercise in addition to celecoxib versus celecoxib alone for symptomatic and radiographic knee osteoarthritis: a randomized controlled trial. BMC Sports Sci Med Rehabil. 2025;17(1):213. doi:10.1186/s13102-025-01263-7.
9. Zeng M, Wu Z, Liang J, Gong A. Efficacy and safety of sodium hyaluronate combined with celecoxib for knee osteoarthritis: a systematic review and meta-analysis. Asian J Surg. 2024;47(3):1331–8. doi:10.37766/inplasy2023.9.0093.
10. Zhou H, Shen X, Yan C, Xiong W, Ma Z, Tan Z, et al. Extracellular vesicles derived from human umbilical cord mesenchymal stem cells alleviate osteoarthritis of the knee in mice model by interacting with METTL3 to reduce m6A of NLRP3 in macrophage. Stem Cell Res Ther. 2022;13(1):322. doi:10.1186/s13287-022-03005-9.

11. Yan J, Jiang S, Ma J, Zhou X, Zhao M, Huang J, et al. Use of the improved tug-of-war acupuncture for promoting cartilage repair by inducing macrophage polarization in knee osteoarthritis. Heliyon. 2024;10(4):e25495. doi:10.1016/j.heliyon.2024.e25495.
12. Xu J, Chen X, Zhang H, Zhang X, Liu R, Li X, et al. Platelet-rich plasma relieves inflammation and pain by regulating M1/M2 macrophage polarization in knee osteoarthritis rats. Sci Rep. 2025;15(1):12805. doi:10.1038/s41598-025-97501-6.
13. Wei J, Liu L, Li Z, Lyu T, Zhao L, Xu X, et al. Fire needling acupuncture suppresses cartilage damage by mediating macrophage polarization in mice with knee osteoarthritis. J Pain Res. 2022;15:1071–82. doi:10.2147/jpr.s360555.
14. Ming C, Bi D, Tian H, Liu W, Li H, Hu Y, et al. Dissolvable microneedles loaded with denosumab alleviate knee osteoarthritis in rodent and canine models by inhibiting macrophage senescence. Theranostics. 2026;16(1):325–44. doi:10.7150/thno.116970.
15. Yi N, Mi Y, Xu X, Li N, Chen B, Yan K, et al. Nodakenin attenuates cartilage degradation and inflammatory responses in a mice model of knee osteoarthritis by regulating mitochondrial Drp1/ROS/NLRP3 axis. Int Immunopharmacol. 2022;113:109349. doi:10.1016/j.intimp.2022.109349.
16. Yuan YS, Li HY, Lu H, Li GC, Cao Z, Xu C, et al. Reprogramming mitochondrial metabolism to enhance macrophages polarization by ROS-responsive nanoparticles for osteoarthritis. Biomaterials. 2025;322:123395. doi:10.1016/j.biomaterials.2025.123395.
17. Wu J, Qin Z, Jiang X, Fang D, Lu Z, Zheng L, et al. ROS-responsive PPGF nanofiber membrane as a drug delivery system for long-term drug release in attenuation of osteoarthritis. npj Regen Med. 2022;7(1):66.
18. Wang Q, Feng K, Wan G, Liao W, Jin J, Wang P, et al. A ROS-responsive hydrogel encapsulated with matrix metalloproteinase-13 siRNA nanocarriers to attenuate osteoarthritis progression. J Nanobiotechnol. 2025;23(1):18. doi:10.1186/s12951-024-03046-7.
19. Li X, Wang X, Liu Q, Yan J, Pan D, Wang L, et al. ROS-Responsive boronate-stabilized polyphenol-poloxamer 188 assembled dexamethasone nanodrug for macrophage repolarization in osteoarthritis treatment. Adv Healthc Mater. 2021;10(20):e2100883. doi:10.1002/adhm.202100883.
20. Shen C, Gao M, Chen H, Zhan Y, Lan Q, Li Z, et al. Reactive oxygen species (ROS)-responsive nanoprobe for bioimaging and targeting therapy of osteoarthritis. J Nanobiotechnol. 2021;19(1):395. doi:10.21203/rs.3.rs-607946/v1.
21. Liu L, Zhang M, Zhou Y, He L, Chen M, Wu Y, et al. An injectable ROS-responsive hydrogel comprising chondroitin sulfate@resveratrol liposome package for osteoarthritis alleviation. Biomaterials. 2025;327:123766. doi:10.1016/j.biomaterials.2025.123766.
22. Wei J, Yang X, Ge X, Zhao L, Liu X, Zhang J, et al. Therapeutic effects of fire needling acupuncture on pain relief and cartilage protection in mia-induced knee osteoarthritis rats: the role of macrophage polarization in synovium and angiogenesis in subchondral bone. J Inflamm Res. 2025;18:7459–75. doi:10.2147/jir.s518829.
23. Ansari MY, Ahmad N, Haqqi TM. Oxidative stress and inflammation in osteoarthritis pathogenesis: role of polyphenols. Biomed Pharmacother. 2020;129:110452. doi:10.1016/j.biopha.2020.110452.
24. Blackler G, Lai-Zhao Y, Klapak J, Philpott HT, Pitchers KK, Maher AR, et al. Targeting STAT6-mediated synovial macrophage activation improves pain in experimental knee osteoarthritis. Arthritis Res Ther. 2024;26(1):73. doi:10.1186/s13075-024-03309-6.
25. Simon L, De Taddeo M, Coeurvolan A, Colpaert M, Richard J, Devoisselle JM, et al. Various lipid anchors on amphiphilic polyoxazolines to reach efficient intracellular delivery. Int J Pharm. 2023;642:123103. doi:10.1016/j.ijpharm.2023.123103.
26. Zhang Z, Lu Z, Yuan Q, Zhang C, Tang Y. ROS-Responsive and active targeted drug delivery based on conjugated polymer nanoparticles for synergistic chemo-/photodynamic therapy. J Mater Chem B. 2021;9(9):2240–8. doi:10.1039/d0tb02996c.
27. Wilson DS, Dalmasso G, Wang L, Sitaraman SV, Merlin D, Murthy N. Orally delivered thioketal nanoparticles loaded with TNF-alpha-siRNA target inflammation and inhibit gene expression in the intestines. Nat Mater. 2010;9(11):923–8. doi:10.1038/nmat2859.

28. Alqahtani MS, Syed R, Alshehri M. Size-dependent phagocytic uptake and immunogenicity of gliadin nanoparticles. Polymers. 2020;12(11):2576. doi:10.3390/polym12112576.
29. Zhen J, Wan T, Sun G, Chen X, Zhang S. A ROS-responsive microsphere capsule encapsulated with NADPH oxidase 4 inhibitor ameliorates macrophage inflammation and ferroptosis. Heliyon. 2024;10(1):e23589. doi:10.1016/j.heliyon.2023.e23589.
30. Ding DF, Xue Y, Wu XC, Zhu ZH, Ding JY, Song YJ, et al. Recent advances in reactive oxygen species (ROS)-responsive polyfunctional nanosystems 3.0 for the treatment of osteoarthritis. J Inflamm Res. 2022;15:5009–26. doi:10.2147/jir.s373898.
31. Luxenhofer R, Han Y, Schulz A, Tong J, He Z, Kabanov AV, et al. Poly (2-oxazoline)s as polymer therapeutics. Macromol Rapid Commun. 2012;33(19):1613–31. doi:10.1002/marc.201200354.